Article

Innovative design of digital neural network-based biodata integration technology in cultural tourism management: Insights from cellular molecular biomechanics perspective

Qingying Zhang[1,*], Yiling Li[2]

[1] College of Culture and Tourism, Zhangzhou Vocational and Technical College, Zhangzhou 363000, China
[2] College of Business, Minnan Normal University, Zhangzhou 363000, China
* Corresponding author: Qingying Zhang, zqy209568@163.com

Abstract: Based on the related feature selection algorithm, this paper builds the basic framework of the multi-strategy method of Fastest Virtual Reality (FVR) feature selection algorithm, and obtains the final collection of biometric data after feature dimensionality reduction and removal of redundant feature values. In the context of cellular molecular biomechanics, the retina sampling network's extraction of pupil biometric features is related to the autonomic nervous system's influence on the iris muscles. The autonomic nervous system, through neurotransmitters and intracellular signaling pathways, regulates the contraction and dilation of the iris, which is reflected in the dynamic change of the pupil diameter. The retina sampling network is established to extract the pupil biometric features in it, and Gabor filtering is applied to extract the image feature data of a small area around a specific point in the image, to obtain the dynamic change data of the visitor's pupil diameter, and combine with the K^* algorithm to evaluate the emotional state of the data segment. Emotional states can affect hormone secretion, such as cortisol and adrenaline, which in turn impact cellular metabolism and neural activity. Use the Radial Basis Function (RBF) network structure model for face biometric data fusion, and according to this method to realize the statistics of attraction foot traffic. The model is applied to the visitor management of a scenic spot, and the emotional state of visitors on holidays is generally higher, among which the highest is 4.2145 on Qingming Festival, and the average pupil diameter of the visitors on that day is also the largest, reaching 3.9615mm.The peak average of the visitor flow of the scenic spot in the morning of the test day is about 44,076 person-times, and the peak average in the afternoon is about 16,254 person-times, among which the average of the flow of the visitors on 2 May is the was the highest, reaching 38,698 person-times. Understanding the cellular molecular biomechanics behind these biometric data helps design more effective strategies to enhance tourists' travel experience.

Keywords: FVR feature selection algorithm; Gabor filtering; RBF network structure model; biometric data; cellular molecular biomechanics

1. Introduction

As an "old" sunrise industry, tourism is rapidly growing worldwide. The impact of tourism on the environment is also gradually being emphasized by the society, and with the increasing call for sustainable use of resources, eco-tourism has emerged as one of the rapidly developing fields in the tourism industry [1,2]. Accompanied by the development of ecotourism and increasingly favored cultural tourism, gradually become an important development trend in the tourism industry attracting attention [3,4].

Biosphere reserves are the earliest form of tourism in China to be established and to introduce the concept of "ecotourism", and they are also an important form of ecotourism service at present. By the end of 2015, China had established more than 2000 nature reserves of various types (429 of which are classified as national level), and 20 of them have been officially approved to join the World Biosphere Reserves [5–8].

With the rise of ecotourism, nature reserves have become the destinations for more and more tourists. Although this trend has raised the importance of people's awareness of nature conservation, it has also brought non-negligible impacts on the ecosystems in protected areas [9,10]. Especially for plant communities, frequent tourism activities may lead to a series of ecological problems such as habitat fragmentation, introduction of invasive species, and changes in plant population structure) [11,12]. Therefore, studying the relationship between tourism activities and plant communities and their diversity in nature reserves is of great theoretical and practical significance for the development of rational tourism management strategies and ecological conservation measures [13]. Biodata integration is a way to measure the changes of individual physiological indicators through bioelectric, which can effectively reflect individual emotional changes.

In China, there are more than 30,000 species of higher plants and 6347 species of vertebrates, accounting for about 10% and 14% of the world's total, respectively, and there are 599 types of terrestrial ecosystems. The Chinese government has actively carried out a series of effective work for biodiversity conservation, including the establishment of a national coordinating mechanism, the strengthening of legislation and law enforcement, the reinforcement of in situ conservation, the emphasis on publicity and education, and the promotion of global cooperation, which has strongly promoted the sustainable development of the national economy and society, and also made important contributions to the conservation of the unique ecosystems, species resources and genetic resources in China [14–16]. In terms of biodiversity conservation, the task ahead is still quite difficult. In order to make regulations more practicable and the establishment of protected areas more scientific and reasonable, it is necessary to provide decision makers and researchers with more scientific and accurate information. However, the amount of biodiversity information is huge, and the structure of the data is complex, with various links between data at different levels. Therefore, how to effectively find the required information resources in this huge amount of data and provide valuable data reference for scientific research and cultural and tourism management is an urgent problem to be solved [17–20].

Nature reserve tourism is an important part of ecotourism, how to ensure the sustainable development of nature reserve tourism and biodiversity has always been the focus of ecotourism management, so the relevant researchers from the perspective of tourists, nature reserve indigenous people, nature reserve management and national policy-making departments to carry out a lot of research. Wolf et al. combined observational and manipulative studies to investigate the impacts of tourists on the natural environment in nature reserve tourism, and analyzed the practical effects of measures such as tourists' travel control, environmental education, and sustainable tourism experiences, which made a positive contribution

to the development of tourism and environmental protection in nature reserves [21]. Chen et al. [22] examined the attitudes of the residents of the reserve towards the development of the Wuyi Mountain National Nature Reserve, and based on the results of the questionnaire survey, it was found that the residents of the reserve showed positive attitudes, and it was pointed out that the education level, gender, and age of the respondents affected their attitudes towards the development of the nature reserve and the development of eco-tourism [22]. Ghoddousi et al. [23] empirically examined how ecotourism development affects biodiversity in Iran's national nature reserves, and the study revealed that from the economic perspective of the communities in the reserves, most of the local residents benefited from tourism development in the nature reserves, and a few suffered economic losses, and the support of most of the residents in the nature reserves was favorable to the development of tourism in the nature reserves and the conservation of biodiversity [23]. Sonbait et al. [24] based on the analysis of official data related to Pegunungan Arfak Nature Reserve (PANR) revealed that the development of PANR is the development of an ecotourism model with the core logic of the local ecological and traditional wisdom, which facilitates the locals to obtain additional economic benefits while ensuring the biodiversity and sustainable development of the nature reserve [24]. Musavengane et al. [25] based on portfolio theory and system resilience theory and using a case study approach in order to discover the optimal integration pathway between social capital and natural resource endowed communities, the study revealed the powerful role of social capital in promoting resilience in nature reserves while arguing that community-based land reforms in nature reserves need to take into account the complexities involved in public natural resources [25]. Mandić et al. [26] systematically reviewed the research literature related to the development of nature reserves, dissected the research results of multi-dimensional nature reserve development governance, construction, visitor management, and monitoring, and at the same time, emphasized the important role of the National Statistical Office(NSO) in promoting the development of tourism in nature reserves, and argued that the relevant practitioners need to have an in-depth understanding of the policies related to the development of tourism in nature reserves [26]. Obradovic et al. [27] investigated how the aborigines of the nature reserve perceived the tourism development of the Uvac Special Nature Reserve, and based on the results of the fieldwork and regression analysis, it was learned that the aborigines of the nature reserve showed active participation in the tourism development of the nature reserve in the hope of realizing their own aspirations while participating in the development of tourism in the nature reserve [27]. Mutanga et al. [28] utilized a questionnaire survey to explore the African wildlife nature reserve visitor experience, tourism motivation and factors affecting the visitor experience, the results of the study showed that the visitor motivation is mainly to get close to nature and wildlife viewing, in which the satisfaction of the visitor's interactions with the wildlife and the perception of the fee significantly affects the visitor's experience satisfaction in the wildlife nature reserve [28].

König et al. [29] illustrated the explosion in the availability of Earth's biodiversity data and conceptualized effective strategies for collecting, inputting, and sharing relevant data and summarized the contemporary frameworks for scalable as

well as biodiversity research, and finally demonstrated a practical case study on the role played by data domains and resolution elements in identifying the biases in global datasets on biodiversity [29]. Heberling et al. [30] provided a systematic overview of research related to global biodiversity data information, noting that the trend in the use of data provided by the Global Biodiversity Information Facility (GBIF) has increased dramatically, with a shift in the direction of research from theory to application, and emphasizing that the integration of biodiversity data and information has been effective in supporting a multitude of interdisciplinary research and applications [30]. Isaac et al. [31] explored biodiversity data integration for summarizing the distribution of species in spatial and temporal dimensions, and introduced a recent biodiversity integration strategy with model as the core logic, which effectively retains the advantages of each biodiversity dataset, and finally discussed in detail through some examples of biodiversity data integration based on big data technologies [31]. Kühl et al. [32] conceptualized a framework for biodiversity data integration through a networked design for coordinating and integrating the efforts of biodiversity monitoring and data collection parties, where the value of combining independent biodiversity observations with a structured core monitoring backbone is consistently emphasized throughout the coordination process, aiming to cultivate broad biodiversity monitoring based on the elements of scientific, societal, policy, and individual ownership and resilience [32]. Scholars have carried out three-dimensional studies from the dimensions of biodiversity data integration pathways, the contribution of biodiversity data to interdisciplinary research and applications, and biodiversity monitoring and data collection, which have promoted the development of research on biodiversity data integration.

In this paper, we associate *T*-test, Relief, Fisher Score, MCFS and other biologically relevant feature selection methods to build a framework based on the multi-strategy approach of the FVR feature selection algorithm, and apply the above algorithms to carry out large-scale feature dimensionality reduction in the biometric feature space, and subsequently combine the feature sets of the performance of different filtered feature selection algorithms through the aggregated voting strategy to obtain the final set of. Construct a pupil sampling network, decompose the dynamic data of pupil diameter in tourists' biometric features by Gabor filtering, and use K^* algorithms to assess the emotional state of the data segments. Apply the algorithm to scenic services to assess the change of emotional value of tourists through the dynamic change of pupil diameter data. Using the radial basis function network model, the face feature extraction of living beings, the collection of face recognition feature values, and the proposed scenic spot human flow statistics program. The model is applied to the scenic area human flow recognition to realize the real-time monitoring of the change trend of the scenic area visitor flow and congestion.

2. Feature selection algorithm FVR for biodata integration based on multi-strategy approach

2.1. Relevant feature selection

2.1.1. *T*-test

T-test is usually used for high-dimensional small sample biological data feature selection link, it is through the detection of the mean value between different groups of variables to study the degree of significant difference, and to determine whether the difference is more significant, *T*-test often need to test the data in line with the law of normal distribution [33]. Usually *T*-test is divided into single overall test and double overall test two ways:

1) Single overall *T*-test: It assesses whether they are significantly different by comparing the sample mean with the group mean, and the specific test formula is as follows:

$$t = \frac{\bar{X} - u}{\frac{\sigma_x}{\sqrt{n}}} \tag{1}$$

where $\bar{X}$ refers to the sample mean, u refers to the group mean, σ_x is the standard deviation of the overall data, and n is the number of data.

2) Dual overall *T*-test: It assesses whether they are significantly different by comparing the sample means between the individual data, and the specific formula for calculating the test is as follows:

$$t = \frac{\bar{X}_1 - \bar{X}_2}{\sqrt{\frac{(n_1-1)S_1^2 + (n_2-1)S_2^2}{n_1+n_2-2}\left(\frac{1}{n_1} + \frac{1}{n_2}\right)}} \tag{2}$$

where $\bar{X}_1$ and $\bar{X}_2$ denote the mean of the different groups of samples, $\bar{S}_1$ and $\bar{S}_2$ denote the variance of the two groups of samples, and n_1 and n_2 denote the number of different samples of data, respectively.

2.1.2. Relief

The Relief algorithm is trained by looping through m randomly selected instances (R_i) with m specific values set by human [34]. During each loop, each instance R_i serves as a target instance, and the specific values of the feature weights matrix W are updated by the observed feature differences between the target instance and the nearest neighbor instances, so that the distances between the target instance and the other instances are computed in each loop. The nearest neighbor instances of the target instance R_i are divided into two types, where the nearest neighbor samples with the same type are called NearHit, and the nearest neighbor samples with different types are called NearMiss. the distance between a feature data in the target instance R_i and the data point NearHit of the same kind and the nearest neighbor indicates the degree of redundancy of the feature, and if the value is less than the distance between the data points with different kind and nearest neighbor NearMiss, then it indicates that the redundancy of the feature is low and the weight parameter of this feature data should be enhanced, and vice versa, the weight parameter of this feature data should be reduced.The update function of the feature weight matrix of the Relief algorithm is shown below:

$$W(f_1) = W(f_1) - \frac{Diff(f_i, P_i, H_j)}{m} + \frac{Diff(f_i, P_i, M_j)}{m} \tag{3}$$

where P_i is a randomly selected sample, H_j is the nearest neighbor sample of the same class, and M_j is the nearest neighbor sample of a different class, the $Diff$ function reflects the difference between different samples in a certain characteristic, and its expression formula is:

$$Diff\left(i, S_1, S_2\right) = \begin{cases} \dfrac{\left|S_{1[i]} - S_{2[i]}\right|}{i_{\max} - i_{\min}} & \text{When feature } i \text{ is a continuous feature} \\[2em] 0 & \text{When the feature } i \text{ is the dissociative} \\ & \text{chaacteistic and } S_{1[i]} = S_{2[i]} \\[1em] 1 & \text{When the feature } i \text{ is the dissociative} \\ & \text{characteistic and } S_{1[i]} \neq S_{2[i]} \end{cases} \qquad (4)$$

2.1.3. Fisher score

FisherScore algorithm is based on the idea of filtering approach to accomplish the task of supervised feature selection by calculating the weight coefficients of all the features, and it is also a classical univariate filtering approach, which consists of the tester setting a threshold or correlation coefficient as an evaluation criterion, and then obtaining a subset of the features according to the penalty function [35]. It aims to find a feature subset that meets the requirement of maximizing the spacing between different classes of data and minimizing the spacing between the same class of data, which is reflected by the FisherScore, whose larger value indicates that it meets this requirement. Therefore, the specific approach for feature selection is to use FisherScore to calculate the weight score of each feature, and then sort all the gene features in descending order of their scores to filter the features, assuming that the initial gene expression matrix is $X \in \mu^m \times n$, which has c different classes, and the specific formula for calculating the FisherScore of the i rd feature is as follows:

$$S_b(f_m) = \sum_{k=1}^{c} d_k \left(\mu_m^{(k)} - \mu_m\right)^2 \qquad (5)$$

$$S_i^{(k)}(f_m) = \sum_{n=1}^{n_2} \left(x_{mn}^{(k)} - \mu_m^{(k)}\right)^2 \qquad (6)$$

$$FS(f_n) = \frac{S_b(f_m)}{\sum_{k=1}^{c} S_t^{(k)}(f_m)} \qquad (7)$$

where $S_b(f_m)$ represents the divergence between different classes of the m trait, d_k represents the number of data in the kth category, $\mu_m^{(k)}$ represents the mean gene expression of the mth trait in the k th category, μ_m represents the expression value of the mth gene of the kth category mean species, $S_i^{(k)}(f_m)$ represents the divergence of

the mth trait within the same class in the kth class, and $x_{mn}^{(k)}$ represents the expression of the mth gene in the nth sample of the kth species.

2.1.4. MCFS

The MCFS algorithm is the earliest filtered unsupervised feature selection method based on spectral analysis and sparse learning methods, which consists of three main steps:(1) Spectral analysis: Firstly, spectral analysis is applied to the original dataset in order to detect the clustering structure of the data; (2) Sparse coefficients learning: Due to the embedded clustering results of the data are known, MCFS draws on the first k features in the Laplacian matrix in order to pass the features with an L1 paradigm regularization of the model to measure the importance of the features; (3) MCFS selects d features based on the highest value of the absolute value of the obtained coefficients [36].

where the thermal weighting matrix between connected nodes is:

$$W_{ij} = e^{-\frac{\|x_j - x_j\|^2}{\sigma}} \tag{8}$$

The Laplace equation for the computational map is:

$$L = D - W \tag{9}$$

D in Equation (9) is a pairwise matrix, defined as $D_{ij} = \sum_j W_{ji}$, which has dimensions comparable to the thermal weighting matrix.

The formula for solving the generalized eigenvalue problem in the pseudo-code:

$$Ly = \lambda D y \tag{10}$$

Equivalent formulas for regression problems:

$$\begin{aligned} min\|y_k - X^T a_k\|^2 \\ s \times t \times |a_k| \le \gamma \end{aligned} \tag{11}$$

The formula for calculating the MCFS score for each feature:

$$MCFS(j) = max|a_k, j| \tag{12}$$

2.2. Integration methods

Integration method is a method to obtain a set of feature subsets by aggregating the results from multiple sets of ensembles, which can well solve the instability problem of feature selection algorithms [37]. Integration methods contain many kinds of strategies to run a specific feature selection algorithm in multiple subsamples and then combine the multiple feature subsets obtained by some means of aggregation to obtain a more stable feature subset.

2.3. Integration features based on a multi-strategy approach

2.3.1. Algorithmic framework

Figure 1 shows the framework of the multi-strategy approach of the FVR feature selection algorithm. It presents the specific implementation process of the three strategies in the FVR algorithm. The hybrid filtered feature selection strategy

aims at large-scale feature dimensionality reduction in the feature space, followed by the aggregation voting strategy to obtain a feature set that combines the performance of different filtered feature selection algorithms, and finally the recursive feature removal strategy to further sift out the redundant features to obtain the final set of features.
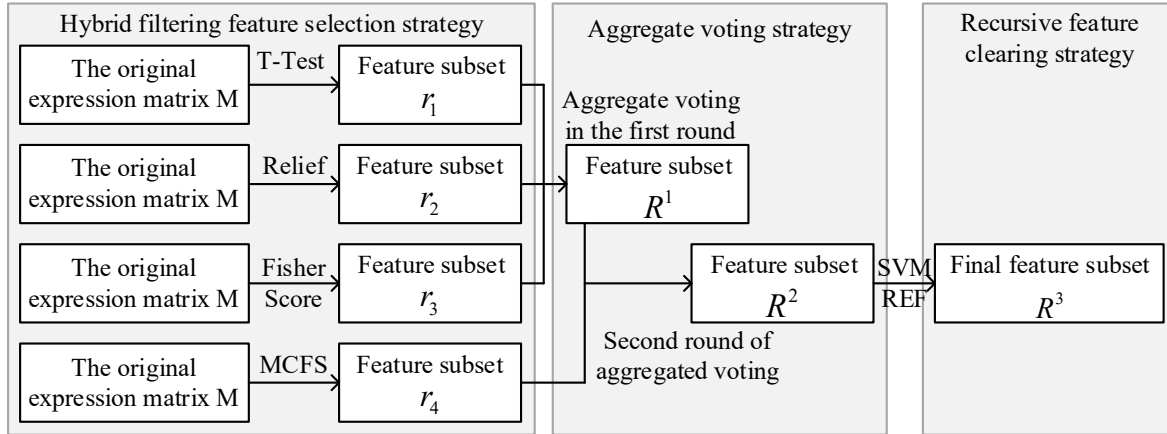

Figure 1. Frame diagram of FVR feature selection algorithm multi-strategy approach.

2.3.2. Filter layers

1) Hybrid filtered feature selection strategy

In this study, the proposed hybrid filtered feature selection strategy combines the advantages of supervised and unsupervised filtered algorithms by using four different filtering methods-*T*-test, Relief, Fisher-Score and MCFS. Since each method uses different criteria, the They can select different subsets of features and produce different classification success rates, and finally the different subsets are combined by an aggregated voting strategy to form the final set of features in the filtering layer.

2) Aggregate voting strategy

Usually, a simple voting or majority voting strategy can be used, i.e., selecting features with more than two votes or selecting several features with the most votes. Considering that there are different feature selection algorithms based on different principles in the hybrid filtering feature selection strategy, it is difficult to eliminate the differences between different classes of algorithms in the "simple and rough" majority voting strategy or simple voting strategy, so combining with the ideas of the previous researchers, we propose an aggregated voting strategy here. In short, we can set a voting committee, where the number of members is the number of participating algorithms, and set different voting thresholds for different scenarios.

2.3.3. Parcel layer

1) Support Vector Machine

Support vector machine ensures classification accuracy by adopting the principle of minimizing structural risk, reducing empirical error and VC confidence range to improve the generalization performance of the model. It is based on the principle of seeking the optimal classification hyperplane $\omega^T x + b = 0$ so that the classes possess maximized geometric intervals between them. Where ω is the

weight vector parameter of the optimal classification hyperplane and b is the deviation. It is desired that the optimal hyperplane obtained by the support vector machine model maximizes the classification interval between two classes and guarantees the accuracy of the classification. We need to solve the following equations to obtain the weight vector parameters and the deviation:

$$min\frac{1}{2}\|\omega\|^2 + C\sum_{i=1i}^{N}\zeta_i \tag{13}$$

$$s.t.\, y_i(\omega \times x_i + b) \geq 1 - \zeta; i = 1,2,\dots,N \\ \zeta_i \geq 0; i = 1,2,\dots,N \tag{14}$$

where: C is the penalty factor and ζ is the slack variable.

The optimization problem of a support vector machine is in essence actually an inequality constrained optimization problem, and the Lagrange multiplier method can be introduced to transform the optimization problem of a support vector machine into solving the following dyadic problem:

$$min\frac{1}{2}\sum_{i=1}^{N}\sum_{j=1}^{N}\alpha_i\alpha_j y_i y_j(x_i \times x_j) - \sum_{i=1}^{N}\alpha_i \tag{15}$$

$$s.t.\sum_{i=1}^{N}y_i\alpha_i = 0; 0 \leq \alpha_i \leq C, i = 1,2,\dots,N \tag{16}$$

where α_i is the Lagrange multiplier, there is the following correlation between the parameters of the weight vector and the formula for solving the dyadic problem:

$$\omega = \sum_{i=1}^{N}\alpha_i y_i x_i \tag{17}$$

where the samples located at the edges follow $0 < \alpha_i \leq C$, C is a constant value.

The discriminant function of the support vector machine model is:

$$f(x) = sgn\left(\sum_{i=1}^{N}\alpha_i y_i x_i \times x + b\right) \tag{18}$$

where $sgn(\cdot)$ is the mathematical sign function.

2) Recursive feature elimination strategy

In the FVR feature selection algorithm model, a support vector machine-based recursive feature elimination (SVM-RFE) strategy is used for further feature screening to remove historically redundant features to obtain a more accurate subset of best-performing features. In the SVM-RFE algorithm, we define the ranking criterion score of the current i nd feature as:

$$c_i = \omega_i^2 \tag{19}$$

The support vector machine model is first constructed based on the original set of features as a training dataset, and then after sorting the feature set according to

their weight coefficients, the feature with the smallest weight coefficient is removed because it has less influence weight in the support vector machine model. In the next iteration, the support vector machine model is trained based on the current subset of features, which leads to the next iterative process until all the features are removed, and finally all the features are ranked for relevance based on the order in which they are removed. The last removed feature is the top ranked feature and most relevant to the class label.

3. Visitor emotion recognition based on pupil diameter dynamics in biometric data

3.1. Affective assessment of tourists based on pupil dynamic data

3.1.1. Pupil sampling network

A retinal sampling grid as described previously is created in this system model. It can be placed on the eye of the subject. This retinal sampling grid consists of sampling points distributed in concentric circles, with the radius of the innermost circle being one pixel and the outermost one being one pixel. Initially in the system model, the radii of the innermost and outermost layers were empirically derived from two main factors the proportion of the eye region in the picture and the size of the picture itself the other factor was the biological features desired to be included.

3.1.2. Gabor decomposition

1) Gabor filter

When storing image data, there are many ways of storing the representation, the image can be represented as a matrix with the data values being the brightness values of the image data in a Cartesian coordinate system. The image can also be represented as a set of superimposed sinusoids with different frequencies, phases and amplitudes by Fourier transform.

Gabor filtering is an excellent band-pass filter. This filter is obtained by multiplying a Gaussian kernel by a complex sine wave with the following formula:

$$g(t) = ke^{j\theta}w(at)s(t) \tag{20}$$

Here:

$$w(t) = e^{-\pi t^2} \tag{21}$$

$$s(t) = e^{j(2\pi f_0 t)} \tag{22}$$

$$e^{j\theta}s(t)e^{j(2\pi f_0 t + \theta)} = (sin(2\pi f_0 t + \theta), j\, cos(2\pi f_0 t + \theta)) \tag{23}$$

Here all k, θ, f_0 are filter parameters. A Gabor filter can be thought of as two different phase filters smoothly assigned to the real and imaginary parts of a complex function. The real part is shown in the following equation:

$$gr(t) = w(t)\, sin(2\pi f_0 t + \theta) \tag{24}$$

The imaginary part is shown in the following equation:

$$g_i(t) = w(t)\, cos(2\pi f_0 t + \theta) \tag{25}$$

2)   Gabor filter set

Biological experiments have shown that the response of human visual nerve cells to spatial information input is frequency selective and has a certain frequency bandwidth range. The frequency bandwidth here is usually defined by the frequency width when the response amplitude is half of the maximum value (i.e., the half-peak bandwidth). The frequency response bandwidth of human visual nerve cells ranges from 0.5 to 2.5 octaves and can be determined by setting the Gabor filter bandwidth parameters. Due to the bandpass nature of the Cabor filter, the frequency range coincides with the passband of the Gabor filter and the value of the filter output will be large. The opposite will receive suppression. Considering that the vast majority of the energy is concentrated within the effective bandwidth of the filter, in this paper, Gabor energy features are used to characterize the image texture features extracted from the biological dataset.

The tool used for the extraction of features in this model is Gabor filter decomposition. In this paper, the logarithmically polar separable Gabor filter decomposition is used to extract the image feature data from a small region around a particular point in the image. Since the region direction and wave number varies from point to point in the image, multiple Gabor filters are required to accomplish the feature extraction. This set of Gabor filters is also known as the Gabor filter bank. The filters in the Gabor filter bank are designed in the logarithmic polar coordinate domain. This is a logarithmic polar scale space:

$$f(\xi,\eta) = A\, exp\left(-\frac{(\xi-\xi_0)^2}{2\delta^2\xi}\right) exp\left(-\frac{(\eta-\eta_0)^2}{2\delta^2\eta}\right) \tag{26}$$

As shown in Equation (26), the filter function $f(\xi,\eta)$ here is defined in the logarithmic polar frequency domain, and A in the formula is a normalized constant. When the direction in the filter function $f(\xi,\eta)$ is modulated to direction η_0 while the absolute frequency is modulated to ξ_0, then the filter equation degenerates to an absolute angular frequency function $w_0 = exp(\xi_0)$. The logarithmic polar frequency coordinate system is defined by Equation (27) below:

$$(\xi,\eta) = log(|w|), tan^{-1}(w_x, w_y) \tag{27}$$

Intuitively and visually, the Gabor filter is a two-dimensional Gaussian bell curve. In the logarithmic polar domain, the Gabor filter is a symmetric two-dimensional Gaussian bell, but in the Cartesian frequency coordinate system, the Gabor filter is an egg-shaped bell.

After constructing the Gabor filter bank described above, it is possible to compute the response data of the Gabor filter bank at any grid sampling point. The Gabor eigenvector is introduced here, which is ordered in terms of the number and direction of the ansatz waves. An element of this feature vector represents the response magnitude of the corresponding Gabor filter and is calculated by the following equation:

$$k(\xi_0, \eta_0) = \left| \sum_{m=0}^{M-1} \sum_{n=0}^{N-1} IM(m,n)f(m,n,\xi_0,\eta_0) \right| \tag{28}$$

For a sample point P in the image, there is a small region surrounding the P point, and the response magnitude K is the absolute value of the scalar product of the responses of all the filters in the Gabor filter bank and all the points in the small region. The small region is clipped from the original image and given a subscript m, n to access each point within this $M \times N$ image rectangle. A Gabor filter $f(m, n, \xi_0, \eta_0)$ is a two-dimensional complex filter corresponding to its particular frequency ξ_0 and direction 70. Each element of the foregoing feature vector is the absolute value of the scalar product of the points in the small region with a given complex Gabor filter f. The index symbol ξ_0 in the equation refers to the absolute frequency of each filter f. The higher the frequency the smaller the filter. Similarly, η_0 determines the direction of the filter. The spatial dimension of the feature vector at the grid sampling point is determined by the product of the number of channels and the number of directions. Note that in Equation (28), the small region IM and filter f are computed in the spatial domain as a scalar product. ξ_0 and η_0 do not represent actual frequency or direction values, but only an index number of the applied channel (the response of a particular filter).

3.1.3. Emotional assessment based on dynamic numerical analysis of pupil diameter

Although the trend of pupil change due to mood fluctuation has significant features, there is individual variability in the participants' pupil signals, so in order to unify the criteria for feature extraction, all the denoised samples need to be normalized as shown in Equation (29), where $y(t)$ and $y'(t)$ are the original and normalized signals, respectively:

$$y'(t) = 2 \times \frac{y(t) - y_{min}}{ymin_{max} - 1}, t = 1, 2, \ldots, N \tag{29}$$

Whenever there is a sudden change in a subject's affective state, the pupil diameter tends to rise abruptly or flutter violently, and the mean and variance of a specific time period also increase significantly, all of which can be used as a feature to distinguish calm from other affective states. In order to capture these characteristic transitions as markers of emotional state differentiation, this study performed a Walsh transform of the data for frequency domain analysis (a total of 180,000 pupil diameter values were obtained from a three-minute-long eye-tracker acquisition at a sampling frequency of 1000 Hz).

The one-dimensional Walsh transform function is defined as shown in Equation (30):

$$W(u) = \frac{1}{N} \sum_{t=0}^{N-1} y(t) \prod_{i=0}^{n-1} (-1)^{b[i](t) \times b[n-1-i](u)} \tag{30}$$

where $u = 0, 1, \ldots, N - 1$, is the index of the Walsh coefficients, $W(u)$ is the u rd coefficient obtained from the Walsh transform indicating the magnitude of the u th

component in the frequency domain. $y(t)$ is the one-dimensional time series to be transformed, and $b[k](u)$ is the k th in the binary representation of index u .

3.1.4. Classification algorithms

In this study, machine learning techniques are used to assess the emotional state of data segments.

$K^{\times}$: The algorithm uses entropy theory as its core foundation and is an improvement of the k Nearest Neighbor (KNN) algorithm, which is mostly used for pattern recognition and data mining. In this algorithm, the distance measure between samples is computed with the help of a probabilistic framework, which calculates the transition probability from one sample to another by randomly selecting all possible transition paths. Given a test object x of unknown category, $K^{\times}$ the algorithm computes the transition probability between the test object x to a member sample n of each category C in the training set:

$$P^{\times}(C|x) = \sum_{n \in C} P^{\times}(n|x)$$

(31)

Finally, the category with the highest probability is selected as the classification result of the test object. $K^{\times}$ algorithm introduces the ideas of probability and entropy theory on the basis of KNN, which provides a more in-depth and comprehensive solution to the classification problem.

3.2. Dynamic emotion assessment based on pupil diameter

3.2.1. Changes in tourists' emotions

Using the pupil diameter dynamic change data in the biological dataset, the emotional time change of tourists was analyzed using HS tourist attractions as an example. **Figure 2** shows the relationship between the emotional value of tourists in HS scenic spots and the change of pupil diameter data. Humans are in excitement or fear: Pupil dilation, relaxation or sadness: Pupil narrowing, and the diameter of the pupil ranges from 2.5 to 4 mm.

The analysis of temporal changes in tourists' emotions is mainly based on the unit of month, week and holiday to study the change characteristics shown by tourists' emotions under different time scales. The average annual sentiment value of tourists is 3.62345, which is in the range of generally positive sentiment values.

Taking the month as a unit, comparing the mean value of the emotion of each month with the change of pupil diameter data, the statistics of the average value of the emotion of tourists in each month showed that the fluctuation of the monthly change was more obvious, with the fluctuation range of [3.2936, 3.8166], and the extreme difference of 0.523, which showed the trend of the wave-like change. Visitor sentiment was higher in March (3.7156) and November (3.8166) and lower in July (3.2936).
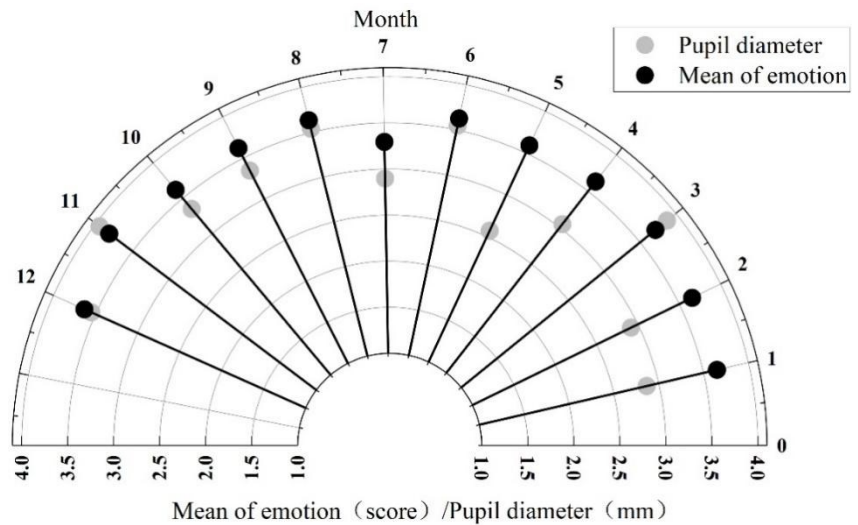
Figure 2. Data changes of visitor's emotional value and pupil diameter.

Figure 3 shows the weekly relationship between tourists' emotion and pupil diameter data. The mean value of emotion ranges from [3.5163,3.7262], with an extreme difference of 0.2099, indicating that tourists' emotion is not affected by the days of the week. The change of pupil diameter data during the week was in the shape of "U", with larger pupil diameters on Saturdays, Sundays and Mondays, indicating that tourists' emotions were excited. Therefore, weekends and Mondays receive more tourists.
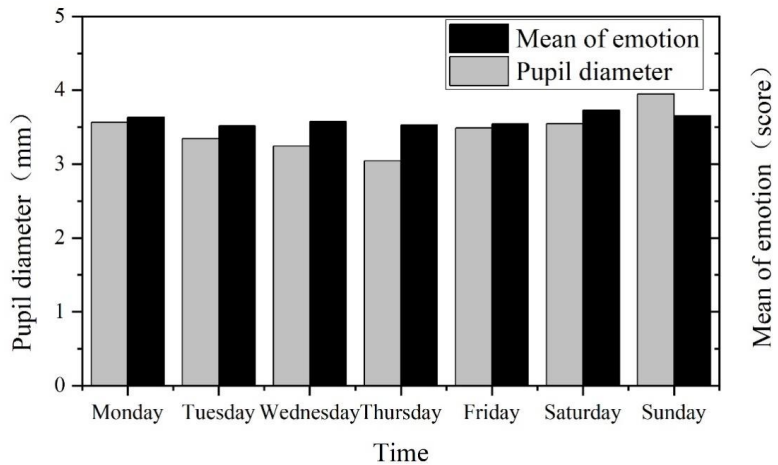

Figure 3. The relationship between visitor emotion and pupil diameter data.

The emotional changes of tourists on holidays were analyzed, taking the seven national legal holidays of New Year's Day, Spring Festival, Qingming, May Day, Dragon Boat Festival, Mid-Autumn Festival and National Day as an example, and the relationship between the average value of tourists' emotions and the change of pupil diameter during the holidays were counted respectively, as shown in **Figure 4**, the emotional state of tourists in the holidays was generally higher, among which the Qingming Festival was the highest, reaching 4.2145, and the average diameter of tourists' pupil on that day was also was the largest (3.9615 mm).
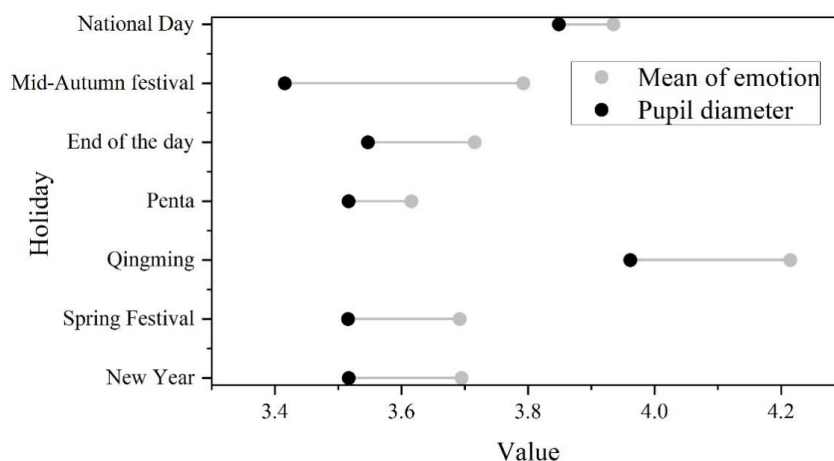
Figure 4. Changes in the mood of tourists and pupils' diameter data.

3.2.2. Spatial distribution of tourists' emotions

In order to make clearer the hotspots where tourists express their emotions, the pupil diameter data of tourists within each square grid is sorted in descending order, and the top 10 areas with pupil diameters are shown in **Table 1**, which are frequented by tourists and contain 4 types of attractions, boutique hotels, commercial streets and entrances and exits. From the mean value of emotion, the emotion of tourists in attractions is higher than that of other three types, and the top three areas in terms of emotion value, namely, the ancestral temple (3.9264), the Banyan Tree (3.7165), and the bazaar life neighborhood (3.6728), are all based on the main characteristics of the buildings (clusters), and their styles are more consistent.

Table 1. The spot emotional value hotspot area statistics.

Serial number	Region	Emotional mean
1	Bird watching pavilion	3.6489
2	Underwater eco-tourism corridor	3.2654
3	Groggery	3.4355
4	Fishing boat route	3.6188
5	Banyan Tree	3.7165
6	Market living block	3.6728
7	Clan hall	3.9264
8	Guesthouse	3.5965
9	North Gate ticket office	3.3948
10	Entrances and exits	3.5615

3.3. Perception optimization services based on tourists' emotions

Scenic spots should shift from "service" to "operation". When tourists in the scenic area on the activities of more and more vigorous demand, the scenic area can not still only provide simple beautiful landscape for tourists to take pictures. Under the new leisure era, the planning and design of scenic spots need to be updated, and the management mode also needs to be transformed. Urban scenic areas should provide tourists with a variety of activities possible, but also can realize the

economic benefits of income generation, for example, Xixi National Wetland held a variety of folklore, cultural activities held in a long period and rich in content, all year round, always let the tourists to maintain a high level of positive emotions. Standardize the behavior of tourists to create a civilized scenic area. National quality more and more high today, few scenic spots are still littering for tourists headache. Scenic spots should vigorously promote civilized tourism, to tourists to visit the notes of the Special Park. Improve the details, people-oriented, enhance visitor satisfaction. Can be built based on social media big data of urban scenic spots tourists emotional characteristics of the study set up roadside guidance, map printing and other stronger indicative signage system to reduce the probability of getting lost, put anti-mosquito lamps or chemical agents to reduce the number of mosquitoes, set up a real-time weather forecast sign to remind tourists to pay attention to the avoidance of rain, snow. Through the accumulation of small details, the achievement of visitor satisfaction experience.

4. Application of bio-data integration for passenger flow monitoring in scenic spots

4.1. Face recognition based people flow monitoring in scenic spots

4.1.1. Radial basis function network data fusion

Data fusion is the most important step in multi-biometric identification. Neural networks have been successfully applied in different data fusion domains due to their own characteristics. The identification technique of feature layer fusion requires the association of feature vectors extracted from different sensors. Since the types of sensor output data often vary greatly, it is difficult to nonlinearly correlate different types of data and form a fusion vector. Neural network has this special function, it can realize a special nonlinear transformation, the input space into the hidden layer of the space, can make the subsequent classification problem in this space becomes easier. This transformation maximizes a special feature extraction criterion and can be regarded as a special feature extractor. Therefore, neural network is used as a fuser of multi-biometric features.

Among all the neural network models, the radial basis function (RBF) network model has been widely used for its advantages of simple structure and good classification. The structure of the RBF network is shown in **Figure 5**, which is a two-layer network, in which the role of the hidden layer unit is equivalent to a transformation of the input pattern, which transforms the low-dimensional pattern input data into a high-dimensional space for classification and recognition of the output layer, and its transformation role can actually be regarded as feature extraction of the input data.
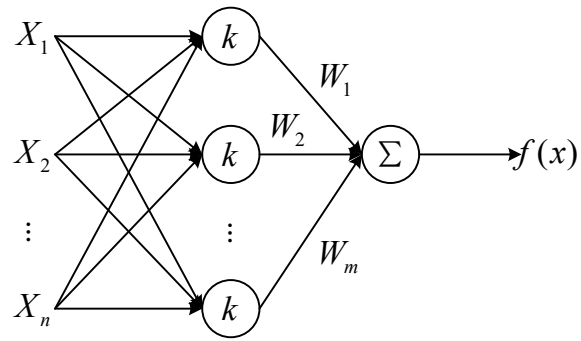
Figure 5. RBF network structure.

The RBF hidden unit uses a nonlinear transfer function. Here, assuming that the transformation function of the RBF hidden unit is the commonly used Gaussian function, the output corresponding to its i st unit is:

$$Z_i(t) = K(|x_j(t) - s_i|) = exp\left[-\frac{\sum_{j=1}^{N}(x_j(t) - S_i)^2}{2a_i^2}\right] \tag{32}$$

where $Z_i(t)$ is the output of the i nd hidden unit (i.e., radial basis function), $x_j(t)$ denotes the jth input mode vector, S_i denotes the transform center vector of the ith unit in the hidden layer, and a_i corresponds to the control parameter of the i th center vector.

4.1.2. Facial recognition program

Facial recognition is a biometric technology for identifying people based on their facial feature information. A camera or webcam is used to capture images or video streams containing faces, and automatically detects and tracks faces in the images, and then performs facial recognition on the detected faces. Face recognition application is to compare and analyze the currently captured face recognition feature values with the stored face recognition feature values through face recognition algorithm.

4.1.3. People counting program

Face feature recognition passenger flow detection method using radial basis function network model to improve statistical accuracy. The target tracker is to track the target detected by the detector to track the center point coordinates of the marker input to the Kalman filter for the prediction of the center point at the next moment. The object bounding box output from the detector is correlated with the inter-frame data to determine the target number. The true center point of the target can be obtained by measuring the obtained center point of the target and the predicted center point of the target. When the target is occluded which may lead to data association failure, the data association can be performed using the tight neighbor optimal tracking algorithm to associate the target at this moment with the target that was occluded just now. If the trajectory abnormality is caused by the obstruction of the target, the trajectory abnormality correction algorithm can be used to correct it.

4.2. Scenic area flow monitoring results

4.2.1. Trends in tourist flow in scenic areas

Using the face recognition-based visitor flow recognition scheme proposed in this paper, the subject scenic area and the monitoring of visitor flow, using SPSS software to HS scenic area in May–June daily 6–20 h of different data sets of visitor flow changes to produce a trend graph, as shown in **Figure 6**. The horizontal axis of the figure indicates different moment values, and the vertical axis indicates the number of tourists (person-times), and the other curves within the picture, in addition to the curve of the average value of tourist flow, indicate the change of tourists on different dates at various moments.

Through the results of **Figure 6** can be obtained most of the time within the visitor flow curve performance for the double-peak curve form, the rest of the part of the more single-peak curve, scenic area visitor flow in the morning peak average value of about 44,076 person-times, the afternoon peak average value of 16,254 person-times or so, in the 2 May when the scenic area within the largest number of tourists, the average value of the flow of the day for the 38,698 person-times, followed by the second, 1 May, the flow of people for the 36,083 people.
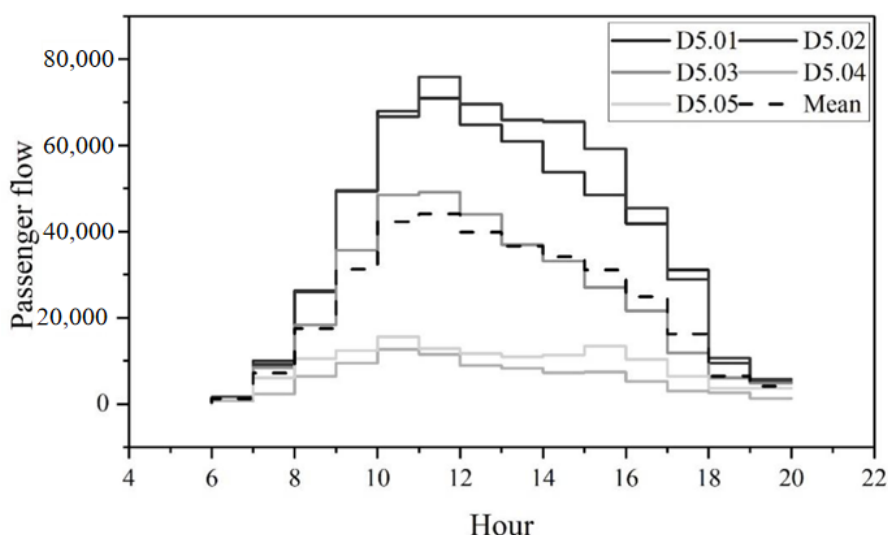

Figure 6. The change trend of tourists in HS.

4.2.2. Analysis of congestion in scenic areas

The model analyzes the changes of scenic congestion under different admission flows. According to the observation statistics, summer weekend night is the peak admission period, the average value is 60 people per minute, corresponding to the average admission time interval is 1 s. Spring and fall weekend morning and afternoon time is the normal admission flow, the average value is 1 person per minute, corresponding to the average admission time interval is 60 s. Taking the average admission time interval as the expectation, we detect the visitors' admission in an exponential distribution. **Figure 7** shows the analysis of scenic congestion, **Figure 7a** is the distribution of visitor spacing under the change of passenger flow, and **Figure 7b** is the distribution of visitor traveling speed under the change of passenger flow.

Figure 7a can be seen, in the park visitors time interval for 60 s, the distance between the tourists show a random distribution, but most of them are maintained in

7.68 m above, the tourists are not much influence on each other, the garden congestion is not obvious. With the gradual shortening of the time interval between visitors, the distance between visitors in the park is gradually shortened, when the time interval between visitors to the park is 1 s, the distance between visitors is mainly concentrated in 1.5–2 m, less than 7.5 m, the visitors began to interact with each other, and the phenomenon of congestion began to appear clearly.

The distribution of tourists' traveling speed is shown by **Figure 7b**. It can be seen that most of the visitors maintain a comfortable traveling speed, i.e., around 1.2 m/s, at the time interval of 60 s between visitors' entry. When the time interval between visitors' entry into the park is 1 s, the speed of visitors' travel begins to show a significant randomized decrease. Visitor flow began to appear unstable phenomena, and signs of congestion gradually became obvious. Interaction between visitors in the park increased during summer holiday evenings.
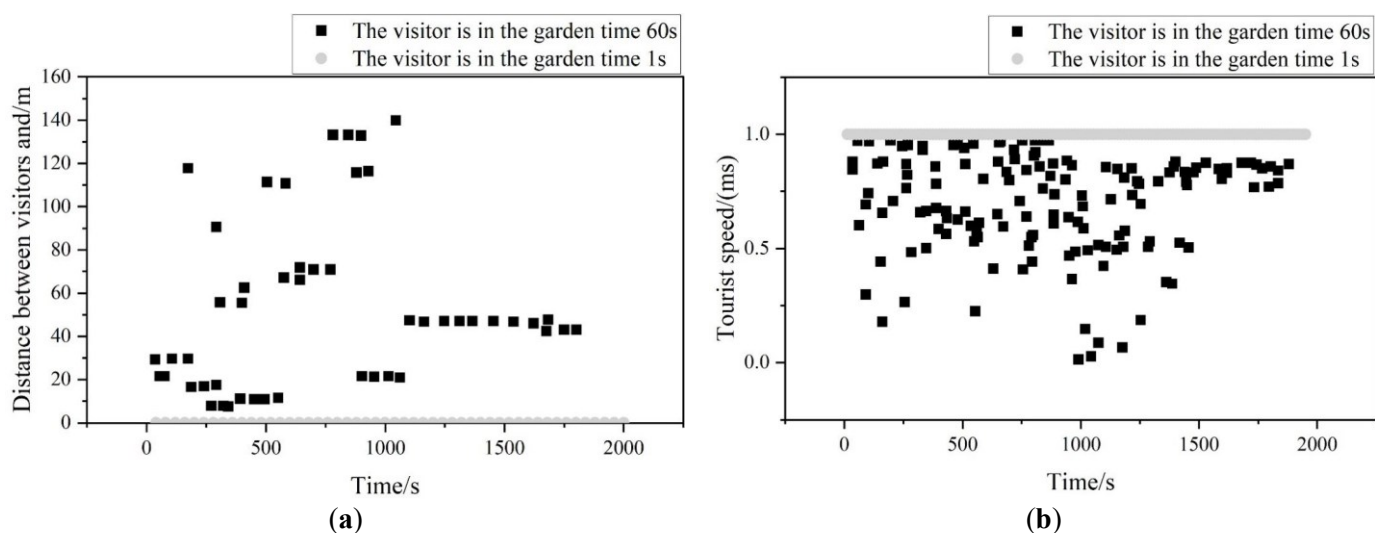

Figure 7. Analysis of congestion in scenic spots. (**a**) Tourist distance distribution under the change of passenger flow; (**b**) tourist travel speed distribution under passenger flow change.

As you can see, the integration monitoring of biometric data can effectively master the tourist data of tourists and provide strong technical support for tourism management planning.

4.3. Tourist flow management optimization recommendations in scenic areas

The above study fully demonstrates that biological data can effectively reflect the characteristics of tourists. This is relatively small in previous studies, and has made outstanding contributions to the research in the academic world. Through the monitoring of individual biological data and the method of face recognition based on machine learning, this paper has integrated an effective tourist management method.

HS scenic area is a special kind of tourism products, and it itself in the management of tourist flow is not perfect, which is inextricably linked with its development and management of the status quo, in order to improve the status quo of localized congestion of tourists, in the following aspects of the adjustment becomes very necessary.

4.3.1. Adjustment of ticketing and verification of scenic spots

The ticketing method of HS scenic spots is now mostly on-site ticketing, or purchasing distributor distribution tickets online and then going to the scenic spots to exchange them for paper tickets for sightseeing. In this smart era of simplicity, efficiency and fast passage, reducing the use of paper tickets can not only achieve the effect of environmental protection, saving manpower, saving the cost of ticketing, but also enable tourists to enjoy more benefits.

Visitor excursion service is a development project of Smooth Tourism Development Limited Liability Company, and its management activities cannot timely cooperate with the efficient management of visitor flow in the scenic spot. It should be coordinated well by the management center of the scenic spot, or jointly with the development company, to optimize the internal ticketing and verification methods of the scenic spot, and to use face recognition technology to mitigate the dense population flow situation through the biometric identification of tourists. Or centralized management of scenic spot ticket sales and internal transportation sales.

4.3.2. Implementation of a real-time booking and flow limitation system

The real-time reservation system is of great significance to the conservation work of the scenic spot and the tourists' visit. Tourists visit the high demand, only the scenic area of the gate only reservation can not control the number of tourists to visit the scenic area. And the scenic area inside the real-time reservation can also limit the flow of tourists can make reasonable arrangements for time. At the same time also make more people can enjoy the scenery under the effective tour distance, so as to meet the deep-seated needs of tourists.

5. Conclusion

In this paper, *T*-test, Relief, Fisher-Score and MCFS algorithms are applied respectively to generate a subset of biometric features and construct a multi-strategy model of FVR feature selection algorithm to realize the integration of biological data. The biometric data of pupil and face are extracted from the biological data set respectively, and the emotional value of tourists and the traffic flow of the scenic spot are detected respectively by using tourists' biological data features. The average annual sentiment value of tourists is 3.62345, which is in the range of generally positive sentiment value, among which the sentiment value of tourists in March and November is higher, which is 3.7156 and 3.8166, respectively. The pupil diameter data of tourists within each square grid were sorted to analyze the spatial distribution of tourists' emotions, and the top three emotional values were Zongzhi, Banyan Tree, and Bazaar Life Neighborhood, with the emotional values of 3.9264, 3.7165, and 3.6728, respectively. Scenic area visitor flow in the morning peak average value of about 44,076 person-times, afternoon peak average value of about 16,254 person-times, the day of 2 May, the largest flow of visitors, reached 38,698 person-times. When the visitors' entry time interval is 1s, the distance between the visitors is mainly concentrated in about 1.5–2m, and the congestion phenomenon begins to appear. Based on the above problems in the scenic area, this paper proposes corresponding management optimization strategies to enhance the tourists' travel experience.

Author contributions: Conceptualization, QZ and YL; methodology, QZ; software, QZ; validation, QZ, and YL; formal analysis, YL; investigation, QZ; data curation, QZ; writing—original draft preparation, QZ; writing—review and editing, QZ; visualization, QZ; supervision, QZ; project administration, QZ; funding acquisition, YL. All authors have read and agreed to the published version of the manuscript.

Ethical approval: Not applicable.

Conflict of interest: The authors declare no conflict of interest.

References

1. Kalaitan, T. V., Stybel, V. V., Gutyj, B. V., et al. (2021). Ecotourism and sustainable development. Prospects for Ukraine. Ukrainian Journal of Ecology, 11(1), 373–383.
2. Hatma Indra Jaya, P., Izudin, A., Aditya, R. (2024). The role of ecotourism in developing local communities in Indonesia. Journal of Ecotourism, 23(1), 20–37.
3. Xiang, C., Yin, L. (2020). Study on the rural ecotourism resource evaluation system. Environmental Technology & Innovation, 20, 101131.
4. Zacarias, D., Loyola, R. (2017). How ecotourism affects human communities. Ecotourism's promise and peril: a biological evaluation, 133–151.
5. Khanra, S., Dhir, A., Kaur, P., Mäntymäki, M. (2021). Bibliometric analysis and literature review of ecotourism: Toward sustainable development. Tourism Management Perspectives, 37, 100777.
6. Martini, U., Buffa, F., Notaro, S. (2017). Community participation, natural resource management and the creation of innovative tourism products: Evidence from Italian networks of reserves in the Alps. Sustainability, 9(12), 2314.
7. Mbaiwa, J. E. (2017). Ecotourism in Botswana: 30 years later. Ecotourism in Sub-Saharan Africa, 110–128.
8. Monz, C., Mitrovich, M., D'Antonio, A., Sisneros-Kidd, A. (2019). Using Mobile Device Data to Estimate Visitation in Parks and Protected Areas: An Example from the Nature Reserve of Orange County, California. Journal of Park & Recreation Administration, 37(4).
9. Thompson, B. S. (2022). Ecotourism anywhere? The lure of ecotourism and the need to scrutinize the potential competitiveness of ecotourism developments. Tourism Management, 92, 104568.
10. Liu, P., Jiang, S., Zhao, L., Li, Y., Zhang, P., Zhang, L. (2017). What are the benefits of strictly protected nature reserves? Rapid assessment of ecosystem service values in Wanglang Nature Reserve, China. Ecosystem Services, 26, 70–78.
11. Turobovich, J. A., Uktamovna, M. N., Turobovna, J. Z. (2020). Marketing aspects of ecotourism development. Economics, (1 (44)), 25–27.
12. Oleśniewicz, P., Pytel, S., Markiewicz-Patkowska, J., Szromek, A. R., Jandová, S. (2020). A model of the sustainable management of the natural environment in national parks—A case study of national parks in Poland. Sustainability, 12(7), 2704.
13. Stronza, A. L., Hunt, C. A., Fitzgerald, L. A. (2019). Ecotourism for conservation?. Annual Review of Environment and Resources, 44(1), 229–253.
14. Ivancsóné Horváth, Z., Kupi, M., Happ, E. (2023). The role of tourism management for sustainable tourism development in nature reserves in Hungary. GeoJournal of Tourism and Geosites, 49(3), 893–900.
15. Ilkhamovna, S. Z., Nodirovna, M. S., Jaxongir, G. (2024). The Experience Of Other Countries In The Legal Regulation Of Agro And Ecotourism. European Journal Of Business Startups And Open Society, 4(3), 112–120.
16. Ma, Z., Chen, Y., Melville, D. S., Fan, J., Liu, J., Dong, J., ... Li, B. (2019). Changes in area and number of nature reserves in China. Conservation Biology, 33(5), 1066–1075.
17. Shumba, T., De Vos, A., Biggs, R., Esler, K. J., Ament, J. M., Clements, H. S. (2020). Effectiveness of private land conservation areas in maintaining natural land cover and biodiversity intactness. Global Ecology and Conservation, 22, e00935.
18. Dube, K., Nhamo, G. (2021). Sustainable development goals localisation in the tourism sector: Lessons from Grootbos private nature reserve, South Africa. GeoJournal, 86, 2191–2208.

19. Arribas, P., Andújar, C., Bohmann, K., DeWaard, J. R., Economo, E. P., Elbrecht, V., ... Emerson, B. C. (2022). Toward global integration of biodiversity big data: a harmonized metabarcode data generation module for terrestrial arthropods. GigaScience, 11, giac065.

20. Vatresia, A., Johar, A., Utama, F. P., Iryani, S. (2020). Automated Data Integration of Biodiversity with OLAP and OLTP. Journal of Information System (e-journal), 7(2), 80–89.

21. Wolf, I. D., Croft, D. B., Green, R. J. (2019). Nature conservation and nature-based tourism: A paradox?. Environments, 6(9), 104.

22. Chen, B. X., Qiu, Z. M. (2017). Community attitudes toward ecotourism development and environmental conservation in nature reserve: a case of Fujian Wuyishan National Nature Reserve, China. Journal of Mountain Science, 14, 1405–1418.

23. Ghoddousi, S., Pintassilgo, P., Mendes, J., Ghoddousi, A., Sequeira, B. (2018). Tourism and nature conservation: A case study in Golestan National Park, Iran. Tourism management perspectives, 26, 20–27.

24. Sonbait, L. Y., Manik, H., Warmetan, H., Wambrauw, Y. L. D., Sagrim, M., Djitmau, D. A., ... Murdjoko, A. (2021). The natural resource management to support tourism: A traditional knowledge approach in Pegunungan Arfak Nature Reserve, West Papua, Indonesia. Biodiversitas Journal of Biological Diversity, 22(10).

25. Musavengane, R., Kloppers, R. (2020). Social capital: An investment towards community resilience in the collaborative natural resources management of community-based tourism schemes. Tourism Management Perspectives, 34, 100654.

26. Mandić, A. (2019). Nature-based solutions for sustainable tourism development in protected natural areas: A review. Environment Systems and Decisions, 39(3), 249–268.

27. Obradovic, S., Tesin, A., Bozovic, T., Milosevi, D. (2020). Residents' perceptions of and satisfaction with tourism development: A case study of the Uvac Special Nature Reserve, Serbia. Tourism and Hospitality Research, 1–13.

28. Mutanga, C. N., Vengesayi, S., Chikuta, O., Muboko, N., Gandiwa, E. (2017). Travel motivation and tourist satisfaction with wildlife tourism experiences in Gonarezhou and Matusadona National Parks, Zimbabwe. Journal of outdoor recreation and tourism, 20, 1–18.

29. König, C., Weigelt, P., Schrader, J., Taylor, A., Kattge, J., Kreft, H. (2019). Biodiversity data integration—the significance of data resolution and domain. PLoS biology, 17(3), e3000183.

30. Heberling, J. M., Miller, J. T., Noesgaard, D., Weingart, S. B., Schigel, D. (2021). Data integration enables global biodiversity synthesis. Proceedings of the National Academy of Sciences, 118(6), e2018093118.

31. Isaac, N. J., Jarzyna, M. A., Keil, P., Dambly, L. I., Boersch-Supan, P. H., Browning, E., ... O'Hara, R. B. (2020). Data integration for large-scale models of species distributions. Trends in ecology & evolution, 35(1), 56–67.

32. Kühl, H. S., Bowler, D. E., Bösch, L., Bruelheide, H., Dauber, J., Eichenberg, D., ... Bonn, A. (2020). Effective biodiversity monitoring needs a culture of integration. One Earth, 3(4), 462–474.

33. Curtis David. (2024). Welch's t test is more sensitive to real world violations of distributional assumptions than student's t test but logistic regression is more robust than either. Statistical Papers(6),3981–3989.

34. Wang Youming,Han Jiali, Zhang Tianqi. (2023). A Relief-PGS algorithm for feature selection and data classification. Intelligent Data Analysis(2),399–415.

35. Wang Zhongyuan,Wang Zijian,Fan Li, Yu Zhihao. (2020). A Hybrid Wi-Fi Fingerprint-Based Localization Scheme Achieved by Combining Fisher Score and Stacked Sparse Autoencoder Algorithms. Mobile Information Systems.

36. Niaz Rizwan,Almanjahie Ibrahim M.,Ali Zulfiqar,Faisal Muhammad, Hussain Ijaz. (2020). A Novel Framework for Selecting Informative Meteorological Stations Using Monte Carlo Feature Selection (MCFS) Algorithm. Advances in Meteorology1–13.

37. Kelsey L. Canada,Tracy Riggins,Simona Ghetti,Noa Ofen, Ana.M. Daugherty. (2024). A data integration method for new advances in development cognitive neuroscience. Developmental Cognitive Neuroscience101475–101475.